Applied Catalysis B: Environmental 92 (2009) 454–461

Contents lists available at ScienceDirect

Applied Catalysis B: Environmental

journal homepage: www.elsevier.com/locate/apcatb

Indoor air purification using heterogeneous photocatalytic oxidation. Part I: Experimental study

Q.L. Yu *, H.J.H. Brouwers

Department of Architecture, Building and Planning, Eindhoven University of Technology, P.O. Box 513, 5600 MB Eindhoven, The Netherlands

ARTICLE INFO

Article history:
Received 15 May 2009
Received in revised form 26 August 2009
Accepted 7 September 2009
Available online 12 September 2009

Keywords:
Heterogeneous photocatalytic oxidation
Indoor air purification
Nitric oxide
Langmuir–Hinshelwood model

ABSTRACT

Heterogeneous photocatalytic oxidation (PCO) has shown to be a promising air purifying technology in outdoor conditions using TiO_2 as photocatalyst activated with UV light. Also to indoor air quality more and more attention is paid because of the very important role it plays on human health, and it can be influenced by many factors like ventilation system, building materials, furniture, cooking, and outdoor pollutants.

The present work addresses the indoor air purification using photocatalytic oxidation. The photocatalytic reaction setup is introduced for the assessment of the indoor air quality. A modified TiO_2 that can be activated with visible light (VIS) is used as photocatalyst due to the shortage of UV light in indoor condition. One special wall paper is applied as the substrate for the coating of the photocatalyst in the present study.

Nitric oxide (NO) is one typical indoor air pollutant, which is used as target pollutant for the photocatalytic oxidation with indoor concentration level. Influential parameters like initial NO concentration, flow rate, relative humidity of the experimental environment, irradiance, photocatalyst dosage that can affect the PCO are studied. Furthermore, the second part content of the present study is introduced at the end of this paper.

1. Introduction

Indoor air quality (IAQ) has received much attention because of the very important role indoor environment plays on human health. Nitric oxides (NO and NO_2), sulfur dioxide (SO_2) and volatile organic compounds (VOCs), as typical inorganic and organic indoor air pollutants, can be emitted from cooking, combustion, exhaust gases, tobacco smoke, furniture, building materials, even traffic pollutants from outside of the building and can cause serious health problem like drowsiness, headache, sore throat, and mental fatigue [1]. The US Environmental Protection Agency (1987) pointed out that indoor air pollution poses a greater risk than outdoor air pollution. So, it is of vital importance to remove these pollutants in order to improve the indoor air quality for people's health.

Traditional methods of reducing indoor air pollution include controlling pollutant sources, increasing the air exchange and using air purifiers. These methods have the following disadvantages. Source control is difficult to achieve in many places. Increasing the air exchange might even transport more pollutants from outdoor environment [2]. Common air purifiers often use sorption materials to adsorb gases or odors which only transfer the contaminants to another phase rather than eliminating them and additional disposal or handling steps are subsequently required.

Heterogeneous photocatalytic oxidation (PCO) has been studied for several decades [3] and shown as an effective method for water or air purification. Some metal oxide semiconductors like TiO_2 and ZnO are commonly used as the photocatalyst in PCO reaction. Among them, TiO_2 is widely used because of its many appropriate characteristics [1]: (a) It is inexpensive, safe, very stable, and has a high photocatalytic efficiency; (b) it promotes ambient temperature oxidation of the major indoor air pollutants; (c) no chemical additives are required. TiO_2 has two main crystal modifications of anatase and rutile with a band gap of 3.2 eV and 2.0 eV, respectively. Anatase has some more superior characteristics than rutile such as the conduction band location is more favorable for conjugate reactions and very stable surface peroxide groups can be formed during PCO reaction which makes it the preferable choice to be used as photocatalyst. However, TiO_2 can only be activated by UV light which is only 0.001–0.05 W/m^2 in indoor illumination [4]. To extend TiO_2 as photocatalyst to visible light region, it is necessary to enlarge the photo absorption of TiO_2 into visible light region (400–700 nm). The usual method is to modify TiO_2 by creating intra-band gap states that are close to the conduction or valence band edges and adsorb visible light at sub-band gap

* Corresponding author. Tel.: +31 40 247 2371; fax: +31 40 243 8595.
E-mail address: q.yu@bwk.tue.nl (Q.L. Yu).

0926-3373/$ – see front matter © 2009 Elsevier B.V. All rights reserved.
doi:10.1016/j.apcatb.2009.09.004

List of symbols

A	area (mm^2)
C	concentration (mg/m^3)
D	hydraulic diameter (dm)
e^-	electron
h^+	electron–hole
H	reactor height (mm)
k	reaction rate constant (mg/m^3 s)
K	adsorption constant (m^3/mg)
L	length (mm)
r	reaction rate (mg/m^3 s)
Q	volumetric flow rate (L/min)
Re	Reynolds number
V	volume (dm^3)
v	linear velocity (m/s)
W	width (mm)

Greek letters

ρ	density (g/m^3)
η_{air}	dynamic viscosity (Ns/m^2)
μ_{air}	kinematic viscosity (m^2/s)

Subscripts

air	air
in	initial concentration
NO	nitric oxide
NO_x	nitric oxide and nitrogen dioxide
out	outlet concentration

energies of less than 3.2 eV such as sol–gel method, doping metal or nonmetal materials onto the surface of TiO_2 [5–10].

Studies on the photocatalytic oxidation of NO_x and VOCs have been carried out intensively. Hoffmann et al. [11] reviewed the environmental applications of semiconductor photocatalysis. Reaction mechanism and kinetics especially using Langmuir–Hinshelwood model were studied; the workability of semiconductor especially TiO_2 and doped-TiO_2 with Fe on PCO was investigated; and photo-reactors for water and air purification were studied with different pollutants. Obee and Brown [1] studied the effect of humidity and pollutants concentration on the oxidation rate of some VOCs with an indoor air level of sub-ppm level. Hashimoto et al. [12] studied the effect of using titania–zeolite composite catalyst for photocatalytic oxidation of NO and found a combination of TiO_2 and zeolite of 7:3 by weight results in a highest PCO rate. Lee and his coworkers [13–15] studied PCO of NO and VOCs in a typical indoor ppb level. The interrelation between NO and VOCs on the PCO effect was studied. The effect of using activated carbon to improve the PCO effect was investigated. Devahasdin et al. [16] studied the reaction kinetics of NO photocatalytic oxidation with an inlet concentration of 20–200 ppm. Ichiura et al. [17] studied the PCO of NO_x using composite sheets containing TiO_2 and metal compounds like CaO and MgO. Results indicate that the CaO treated TiO_2 has the greatest NO_x conversion rate. Jo and Park [18] studied the PCO of VOCs with an inlet concentration of ppb level for indoor air purification and the effect of experimental conditions on photocatalytic oxidation rate was investigated. Pelton et al. [19] studied the photocatalytic paper containing colloidal TiO_2. Wang et al. [20] studied the reaction mechanism of PCO of NO_x with an inlet concentration of 20–168 ppm using TiO_2 supported on woven glass fabric. Kuo et al. [4] studied the PCO of NO_x under visible light using carbon-containing TiO_2 and the effect of the wavelength of the light was investigated. Shelimov et al. [21] studied the enhancement effect of using alumina as support of TiO_2 on the photocatalytic removal of NO_x. Dalton et al. [22] studied the PCO of NO_x using TiO_2 as photocatalyst with a surface spectroscopic approach.

Although great progress has been obtained on the air purification with photocatalytic oxidation, the difference in the findings or conclusions among these studies is still considerable. For instance, in Devahasdin et al. [16], the increase of the relative humidity leads to a higher PCO conversion rate but in Ao and Lee [13] it results in a lower PCO conversion rate. The reaction kinetics of the PCO of NO have been investigated as well, however, as an undesired intermediate, NO_2 was seldom considered in the literature. Thus, further study is still very necessary, especially on indoor air quality improvement as discussed above.

The present research addresses the indoor air purification study with photocatalytic oxidation under indoor conditions. NO was chosen as the target pollutant in the first stage of this study since it is a typical indoor air pollutant that can be emitted from many sources as discussed above. Visible light (VIS) is used as light source in this research, which is different from most literature, among which UV light is still used extensively for the PCO of indoor air purification, although the study of modifying TiO_2 to work in visible light region has been carried out extensively. Here a carbon-doped TiO_2 is used as photocatalyst which is coated onto glass fibers before sprayed onto the wall paper. The experimental study was carried out using the standard ISO 22197-1 [23] as a basic reference. The experimental conditions that influence the photocatalytic oxidation such as light intensity, initial pollutant concentration, flow rate, water vapor, and the amount of photocatalyst were investigated in detail.

2. Experimental

2.1. Materials

A carbon-doped TiO_2 (Kronos, Germany) was used as photocatalyst in the present study. The carbon-doped TiO_2 is produced by mixing a fine grained titanium compound with an organic carbon compound and subsequent thermal treatment at temperatures up to 350 °C [24]. By doping the anatase phase with carbon, the cut-off wavelength is shifted from 388 nm (band gap of 3.20 eV) to 535 nm (band gap of 2.32 eV) which corresponds to bluish green light [25]. The modification indicates that only 2.32 eV needs to be absorbed which means the visible light can be used to activate the powder as photocatalyst. The basic properties of the chosen photocatalyst are shown in Table 1 (values taken from data sheet of provider). Newly designed gypsum plasterboard cover paper with nonwoven glass wool fabric, instead of traditional gypsum paper, was used as substrate for the photocatalyst. This newly designed paper also can be further used as normal wall paper. First slurry was prepared by mixing water with the carbon-doped TiO_2. Then glass fibers were coated by dipping them into the carbon-doped TiO_2 slurry. Finally the glass fibers were sprayed onto the wool fabric with a good adhesion between them after drying.

2.2. Set-up

The schematic diagram of the photocatalytic oxidation set-up used for the PCO of NO for indoor air assessment is shown in Fig. 1. The set-up is developed using ISO standard 22197-1: 2007 [23] as a reference that focuses on advanced ceramics and advanced

Table 1
Physical properties of the used photocatalyst.

Parameter	Photocatalyst
TiO_2 content (ISO 591)	>87.5%
Crystal modification	Anatase
Density (ISO 787, Part 10)	3.9 g/cm^3
Crystallite size	Approximately 15 nm
Specific surface area (BET)	225 m^2/g
Bulk density	>350 g/L
Max. processing temperature	150 °C
Application pH-range	4–9

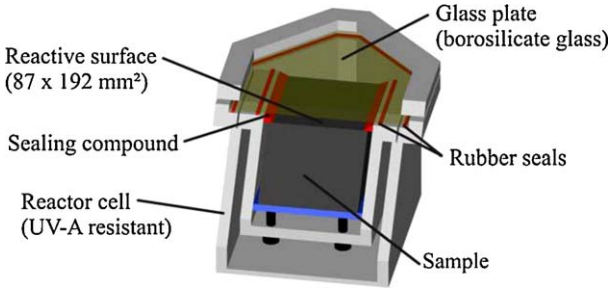

Fig. 2. Schematic diagram of the reactor [26].

technical ceramics. The experimental setup is composed of the reactor, visible light source, target gas pollutant (NO) supply, transport gas supply, analyzer, flow rate valves, relative humidity meter valve, and parameter measurement apparatus like temperature and relative humidity.

The reactor is made from non-adsorbing plastic material with a size of 100 mm × 200 mm ($W \times L$) which allows a planar sample to be embedded shown in Fig. 2 [26]. After placing the testing sample inside, the top of the reactor will be tightly covered with a glass plate made from borosilicate allowing the UV or visible light to pass through with almost no resistance. A more detailed description can be found in Hüsken et al. [26]. The reactor height, which is the distance between the paralleled surface of the testing sample and the covering glass plate, can be adjusted by the screws in the bottom of the reactor. In the present experiments, 3 mm is used as the standard height of the reactor. The target pollutant gas can only pass through the reactor along the longitudinal direction by means of appropriate sealing.

The visible light is used in the experiment. The applied light source consists of three cool day light lamps of each 25 W (Philips, the Netherlands), emitting a visible radiation in the range of 400–700 nm. The irradiance can be adjusted by a light intensity controller. The light intensity is measured with VIS-BG radiometer (Dr. Gröbel UV-Elektronik GmbH, Germany). The VIS-BG radiometer measures a wavelength range of 400–600 nm with the maximum relative sensitivity at around 460 nm. The reason that the VIS-BG radiometer with this measurement range was chosen lies in the characteristics of the photocatalyst used in the experiment. The carbon-doped TiO_2 can be activated in the bluish green light region which is the same as the measurement range of the radiometer. The VIS-BG has a measuring range of 2000 W/m^2 with the resolution of 0.1 W/m^2.

NO is used as target pollutant in the present study. The used gas consists of 50 ppm NO stabilized in nitrogen (N_2). Because of the final target NO concentration ranges in the orders of ppb with the maximum concentration of 1.0 ppm, a transport fluid synthetic air which is composed of 20.5 vol.% oxygen (O_2) and 79.5 vol.% N_2 is deployed, which is humidified by flowing through a demineralized water filled bottle. The target concentration of NO is adjusted by the NO concentration controller and flow rate valves.

Pollutant (NO) and intermediate product (NO_2) were analyzed using a chemiluminescent NO_x analyzer (HORIBA 370, Japan). The analyzer, with a detection limit of 0.5 ppbv, measures the concentration in steps of 5 s while the corresponding NO_x concentration is computed by the difference of the previous two. During the measurement, the analyzer constantly samples gas with the rate of 0.8 L/min.

2.3. PCO experiment

NO is used as target indoor air pollutant in the present research. In a UK study, the average NO_x concentrations were in the range of 9.4–596 μg/m^3 in a weekly average in kitchens for houses with gas cookers, and peak values of up to 3800 μg/m^3 for 1 min have been reported in the Netherlands in kitchens with unvented gas cooking ranges [27]. Based on this, a sub-ppm level of the initial NO concentration was chosen in this research to represent the real indoor air condition, as 1 ppm is about 1.3 mg/m^3 (20 °C, 1 bar).

The photocatalytic oxidation experiments were carried out using a standard procedure illustrated as following. The first step is

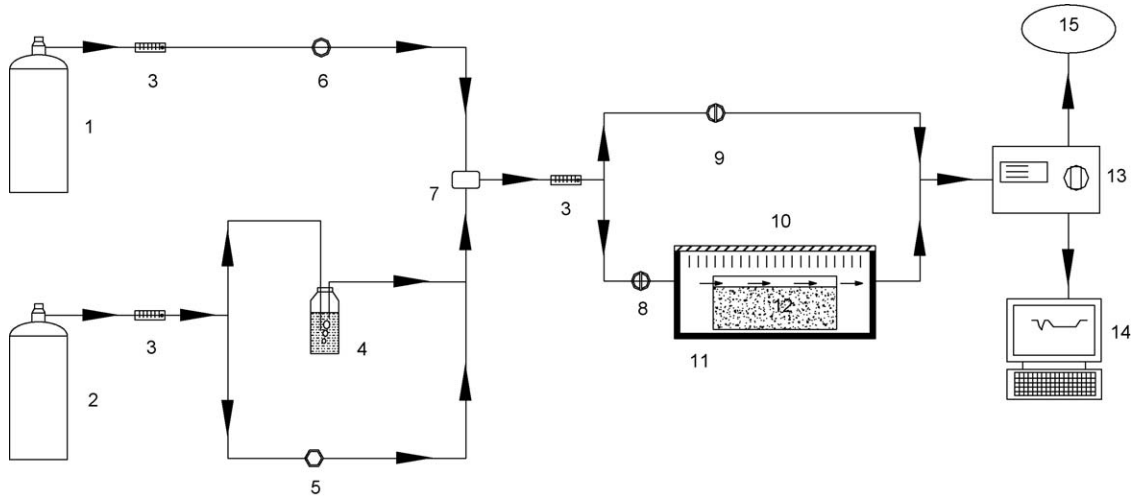

Fig. 1. Schematic diagram of photocatalytic degradation setup. (1) NO gas supply. (2) Synthetic air. (3) Flow rate meter. (4) Humidifier. (5) Humidity controller. (6) NO concentration controller. (7) Temperature and relative humidity sensor. (8) Valve. (9) Valve. (10) Light source. (11) Reaction chamber. (12) Reactor. (13) NO_x analyzer. (14) Computer. (15) Vent.

Table 2
Experimental conditions.

Parameter	Standard conditions	Varying conditions
Reactor Height (mm)	3	2–9
Initial NO concentration (ppm)	0.5	0.1–1.0
Volumetric flow rate (L/min)	3	1–5
Relative humidity (%)	50	10–70
Light intensity E (W/m^2)	10	1–13

to warm up the NO_x analyzer to a stable condition in about 1–3 h, in the present study a 1.5-h warm up time is usually used. In the meantime the reactor is prepared including the preparation of the testing sample, putting the sample into the reactor, sealing the reactor well and putting the reactor into the reaction chamber with the reactor covered. Then the gas supply is allowed to flow through the system using the bypass (with valve 9 open and valve 8 close in Fig. 1), and the concentration is adjusted with the concentration valve while monitored with the analyzer to the desired value. Then the visible light lamp is switched on to get a stable radiation and adjusted to the desired experimental light intensity value with the lamp control valve while the reactor remains covered, followed by the adjustment of the relative humidity to the desired value with the humidity control valve.

When the experimental conditions become stable, the photocatalytic oxidation reaction can be started first by opening the valve 8 and closing valve 9 while keeping the reactor covered. The NO concentration decreases immediately when flowing through the reactor because of the adsorption of NO onto the surface of the sample. Then the concentration increases again to the primary concentration within several minutes, 5–10 min is usually enough in the present research although this value can be influenced by NO initial concentration, flow rate, and the surface structure of the tested sample. This phenomenon also indicates that no photocatalytic oxidation reaction takes place in dark. After this the photocatalytic oxidation reaction is started by uncovering the reactor to allow the visible light irradiate the sample. The photocatalytic oxidation reaction lasts 30 min in the present study and is ended by covering the reactor.

Using the standard ISO 22197-1:2007 [23] as a reference, a standard experimental condition was used in this study. An initial NO concentration was chosen as 500 ppb and the volumetric flow rate of it as 3.0 L/min; the visible light intensity was chosen as 10.0 W/m^2 and a relative humidity of 50%. All the experiments were carried out at room temperature. To study the influence of the experimental conditions on the photocatalytic oxidation rate, the parameters mentioned above were varied to carry out the PCO test, the detailed information is shown in Table 2 and discussed in the following parts.

3. Results and discussion

3.1. Mechanism of photocatalytic NO oxidation

Photocatalytic oxidation can be divided into three main steps: (1) mass transport and adsorption of pollutants from the bulk air to the surface of catalyst; (2) photocatalytic reaction on the catalyst; (3) desorption and mass transport of the reaction products from the surface of catalyst to air. So far the photocatalytic oxidation mechanism has been investigated extensively [6,16,20,22,28]. Based on the present study, a possible photocatalytic oxidation mechanism of NO is proposed using Eqs. (1)–(10):

Eq. (1) shows the photon generation of electron/hole pairs:

$$TiO_2 + h\nu \rightarrow e^+ + h^- \quad (1)$$

Eqs. (2)–(4) show the adsorption of the reactants onto the photocatalyst:

$$TiO_2 + H_2O \Leftrightarrow TiO_2\_H_2O \quad (2)$$

$$TiO_2 + O_2 \Leftrightarrow TiO_2\_O_2 \quad (3)$$

$$TiO_2 + NO \Leftrightarrow TiO_2\_NO \quad (4)$$

Eq. (5) shows the recombination of the generated electron and hole pairs:

$$e^- + h^+ \rightarrow \text{heat} \quad (5)$$

Eqs. (6) and (7) show the trapping of the generated holes and electrons:

$$h^+ + H_2O \rightarrow OH^\bullet + H^+ \quad (6)$$

$$e^- + O_2 \rightarrow O_2^- \quad (7)$$

Eqs. (8)–(10) show the oxidation of NO:

$$NO + OH^\bullet \rightarrow HNO_2 \quad (8)$$

$$HNO_2 + OH^\bullet \rightarrow NO_2 + H_2O \quad (9)$$

$$NO_2 + OH^\bullet \rightarrow NO_3^- + H^+ \quad (10)$$

From these equations it is evident that adsorbed oxygen and water play a very important role in the heterogeneous photocatalytic oxidation reaction. Oxygen is used to trap the generated electrons in the TiO_2 surface. Hydroxyl radicals are produced from water by trapping the generated holes in TiO_2 surface, which then lead to the oxidation of NO_2 and finally NO_3^-. The study of photocatalytic decomposition of NO [8,29] in absence of oxygen and water also indicates their role in the NO photocatalytic oxidation.

3.2. Photocatalytic oxidation of NO

The photocatalytic oxidation reaction takes place immediately when the sample is exposed to the visible light. NO_2 concentration increases and reaches a stable condition quickly. After reaching the maximum degradation rate, the process will slightly slow down and reach a stable conversion condition finally. Fig. 3 shows the concentration change of NO_x during the photocatalytic oxidation reaction.

The photocatalytic oxidation of NO is calculated from Eq. (11) reads:

$$NO_{con}(\%) = \frac{[C_{NO}]_{in} - [C_{NO}]_{out}}{[C_{NO}]_{in}} \times 100 \quad (11)$$

where $C_{NO,out}$ is defined as the average NO concentration of the last 5 min in the measurement time.

Eq. (9) shows the formation of NO_2 during the oxidation reaction. However, not all the produced NO_2 can be oxidized to HNO_3 because a small part of it is released into the air due to desorption. So the exit pollutant is composed of left NO and the undesired intermediate NO_2. The amount of NO_x removed is calculated using Eq. (12) reads.

$$NO_{x_{con}}(\%) = \frac{[C_{NO_x}]_{in} - [C_{NO_x}]_{out}}{[C_{NO_x}]_{in}} \times 100 \quad (12)$$

where $C_{NO_{x,out}}$ is defined as the average NO_x concentration at exit in the last 5 min of the measurement time.

The NO_x conversion is used to study the influence of the different reaction conditions since NO_2 is an undesired intermediate pollutant and it is considered in the present study.

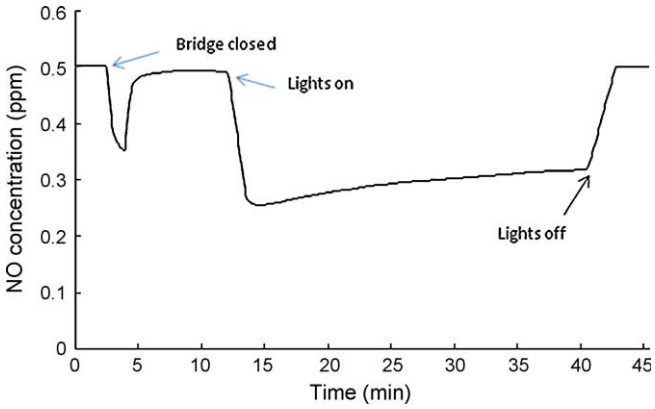

Fig. 3. Schematic diagram of the NO concentration during one PCO test.

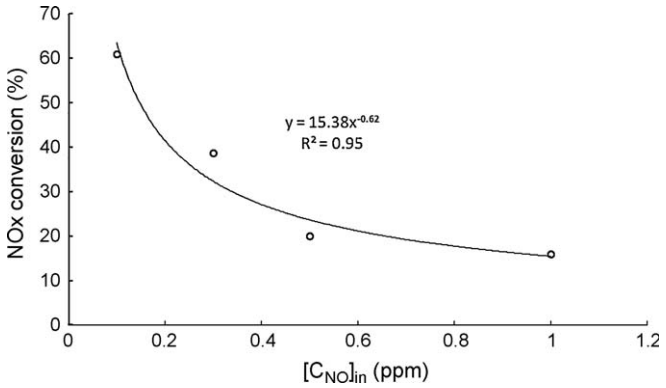

Fig. 4. Effect of the initial pollutant concentration on the NO_x conversion rate (Q = 3 L/min; RH = 50%; I = 10 W/m^2).

Table 3 shows part of the experimental results of NO and NO_x conversion.

3.3. Effect of the initial NO concentration

The level of NO concentration in indoor air environment is in a range of several hundred ppb [13] and can reach to a peak of ppm level in some situations such as a car garage [30]. The photocatalytic oxidation experiments were carried out using different initial NO concentrations ranging from 100 ppb to 1.0 ppm to study its effect on the photocatalytic oxidation rate, while with the standard experimental conditions introduced above.

The effect of the initial concentration on the NO_x conversion rate is shown in Fig. 4. The lower initial NO concentration results in a higher conversion rate. The conversion rate is 60.75% when the initial NO concentration is 0.1 ppm while the conversion rate is only 15.88% when the initial concentration increases to 1.0 ppm, which is also confirmed by Devahasdin et al. [16] who found a conversion of 70% and 15% with the initial concentration of 5.0 ppm and 60.0 ppm, respectively. This probably can be explained by the adsorption ability of the fixed active sites of TiO_2 on the sample surface, which is in accordance with Ao and Lee [14] who reported the NO_x removal rate was improved with the use of activated carbon to help absorb the NO onto the sample surface.

The Langmuir–Hinshelwood model has been widely investigated [1,16,31,32,40] to successfully describe the photocatalytic reaction rate with different pollutants like VOCs and NO. The model employs Langmuir adsorption isotherm to describe the disappearance rate of reactant reads.

$$r = \frac{kKC}{1+KC} \Leftrightarrow \frac{1}{r} = \frac{1}{kKC} + \frac{1}{k} \tag{13}$$

It is clear that the reaction rate in Eq. (13) is first order at low concentration and zero-order at high concentration, which is confirmed by Obee and Brown [1] and Emeline et al. [33]. Yu et al. [34] also reported a linear increase of initial reaction rate at a lower initial concentration of photocatalytic oxidation of formaldehyde in indoor air. So although the conversion of NO is higher with a smaller initial concentration, the lower initial reaction rate means a longer reaction time is needed for the photocatalytic oxidation.

3.4. Effect of flow rate

Varying flow rates results in different photocatalytic oxidation time since it influences the mass transfer and adsorption of NO

Table 3
NO conversion and NO_x conversion results.

E (W/m^2)	Q (L/min)	RH (%)	$C_{NO,in}$ (ppm)	$C_{NO_2,in}$ (ppm)	$C_{NO,out}$ (ppm)	$C_{NO_2,out}$ (ppm)	NO_{con} (%)	$NO_{x_{con}}$ (%)
3	3	50	0.9831	0.0102	0.8773	0.0336	10.77	8.30
5	3	50	0.9755	0.0097	0.8327	0.0412	14.64	11.30
8	3	50	0.9993	0.0116	0.8200	0.0513	17.95	13.82
10	3	50	0.9766	0.0116	0.7791	0.0524	20.22	15.85
13	3	50	0.9805	0.0129	0.7669	0.0582	21.79	16.94
1	3	50	0.4827	0.0047	0.4330	0.0161	10.31	7.87
2	3	50	0.4967	0.0077	0.4089	0.0273	17.68	13.52
4	3	50	0.4933	0.0036	0.3922	0.0296	20.51	15.12
6	3	50	0.4828	0.0036	0.3626	0.0344	24.90	18.37
8	3	50	0.4691	0.0109	0.3419	0.0443	27.12	19.54
10	3	50	0.4933	0.0136	0.3565	0.0493	27.72	19.94
13	3	50	0.4760	0.0162	0.3257	0.0519	31.58	23.28
10	1	50	0.4727	0.0015	0.1416	0.0368	70.03	62.36
10	2	50	0.4876	0.0047	0.2703	0.0480	44.58	35.36
10	3	50	0.4933	0.0136	0.3565	0.0493	27.72	19.94
10	5	50	0.4929	0.0001	0.3991	0.0277	19.03	13.41
10	3	10	0.4895	0.0003	0.4359	0.0110	10.94	8.75
10	3	20	0.4976	0.0045	0.4207	0.0211	15.45	12.02
10	3	30	0.4852	0.0005	0.4003	0.0176	17.49	13.96
10	3	40	0.4964	0.0054	0.3776	0.0349	23.93	17.78
10	3	50	0.4933	0.0136	0.3565	0.0493	27.72	19.94
10	3	60	0.4846	0.0116	0.3064	0.0536	36.78	27.46
10	3	70	0.4859	0.0042	0.2872	0.0493	40.89	31.33

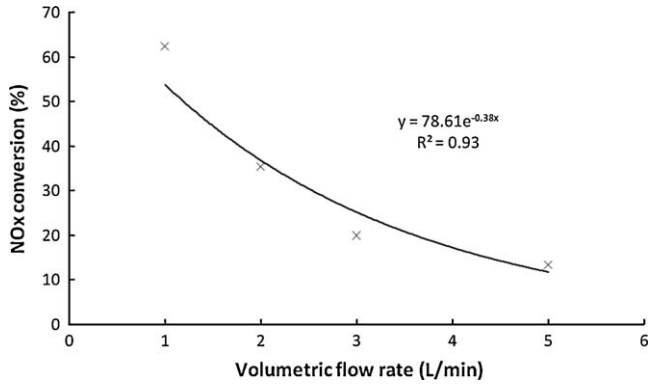

Fig. 5. Effect of the volumetric flow rate on the NO_x conversion rate ($[C_{NO}]_{in}$ = 0.5 ppm; RH = 50%; I = 10 W/m^2).

onto the surface of photocatalyst. Residence time, also known as space time, is defined as the reactor volume divided by the volumetric gas flow rate. Experiments were performed using different volumetric flow rates from 1.0 L/min to 5.0 L/min to study the effect of flow rate. The Reynolds number of the flow that is used to describe the style of the flow reads.

$$Re = \frac{v_{air} D_h \rho_{air}}{\eta_{air}} = \frac{D_h v_{air}}{\mu_{air}} = \frac{4WHQ}{2(W+H)WH\mu_{air}} = \frac{2Q}{(W+H)\mu_{air}} \quad (14)$$

where D_h is defined as 4 times the cross-sectional area ($W \times H$), divided by the wetted perimeter ($2(W+H)$), $\mu_{air} = 1.54 \times 10^{-5}$ (20 °C, 1 bar). Within the used flow rate in the present study, the Reynolds number ranges from 21 to 105, which indicates the flow is laminar.

Figs. 5 and 6 show the photocatalytic oxidation results using the different flow rates. It is evident from the results that the lower flow rate results in the higher conversion. Ao and Lee [13] reported a steady decrease of NO conversion from 88% to 68% when the flow rate increases from 5 L/min to 30 L/min. Devahasin et al. [16] and Wang et al. [20] found the similar effect of the flow rate on the NO conversion that the conversion increases with the increase of the residence time until a value from which the conversion becomes stable, which is different from the present study, in which the results show that the lower the flow rate was, the faster the conversion increase speed was obtained. The system here becomes a batch reactor when the volumetric flow rate decreases to zero, which means a 100% of the conversion will be obtained given a sufficient reaction time. However, the applicable lowest volumetric flow rate is 1 L/min because of the limitation of the test set-up. The influence of the mass transfer between the reactants and photocatalyst was not studied when the flow rate decreases to a very low value.

3.5. Effect of light source

UV light is extensively used to activate the photocatalytic oxidation reaction. With enough activation energy provided by photons from UV light, the electron and holes pairs will be generated on the catalyst surface, which leads to the photocatalytic oxidation of pollutants. The light intensity influences the PCO effect because the number of the produced photons become higher when the light intensity becomes stronger.

Egerton and King [35] pointed out that the PCO rate increases with the light intensity with the first order at low value while half order at high value, which also was confirmed by Herrmann [36] who reported a turning point of the light intensity of 250 W/m^2. The reason is that in the first regime, i.e. first order regime, the generated electron–hole pairs are consumed more rapidly by PCO reaction than by recombination, whereas in the second regime the recombination rate is dominant which results in a decrease of the photocatalytic oxidation. Kim and Hong [37] reported a linear increase of the PCO rate with the increase of the UV light intensity within 40 W/m^2 using VOCs like TCE and toluene as pollutants. This is in line with Yu et al. [34] who reported a linear increase of the PCO conversion of formaldehyde with the increase of the light intensity from 0.5 W/m^2 to 2.5 W/m^2. Devahasdin et al. [16] found a combination effect of NO initial concentration on its conversion with the light intensity varying from 20 W/m^2 to 70 W/m^2, the conversion does not change with an initial concentration of 5 ppm while increases steadily with an initial concentration of 40 ppm.

Visible light was used as light source for the photocatalytic oxidation of NO in the present study using the carbon-doped TiO_2 as photocatalyst research considering the extremely low UV light intensity in indoor condition. By doping with carbon, the band gap between valence bands and conduction bands of TiO_2 was modified which allows its activation by the visible light in bluish range. However, to the authors' knowledge, no study has been carried out on the effect of the visible light intensity on the PCO of NO. A variety of 1.0–13.0 W/m^2 of the visible light intensity was used in the present research to study its effect of the photocatalytic oxidation rate. The results are shown in Fig. 7. The NO_x conversion rate increases with the increase of the light intensity according to a logarithmic relation, which is different from all the available literature. The NO_x conversion rate increase has the same logarithmic rule with the increase of the light intensity using

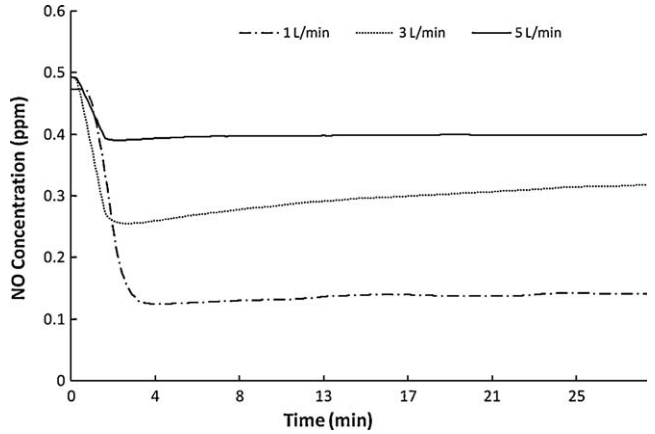

Fig. 6. Diagram of NO concentration change during measurement with different volumetric flow rates.

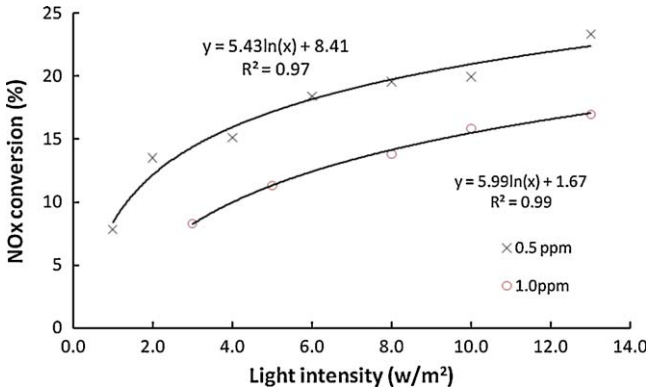

Fig. 7. Effect of light intensity on the NO_x conversion rate ($[C_{NO}]_{in}$ = 0.5 ppm; Q = 3 L/min; RH = 50%). .

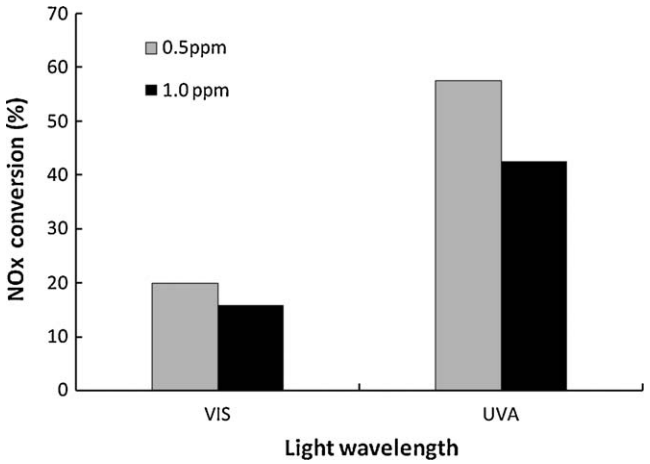

Fig. 8. Effect of light wavelength on the NO_x conversion rate ($[C_{NO}]_{in}$ = 0.5 ppm; Q = 3 L/min; RH = 50%; I = 10 W/m^2).

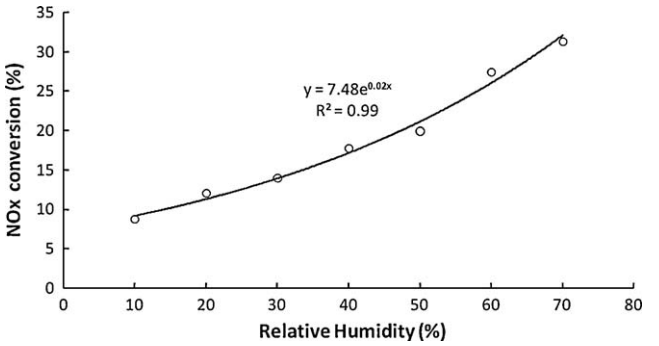

Fig. 9. Effect of the relative humidity on the NO_x conversion rate ($[C_{NO}]_{in}$ = 0.5 ppm; Q = 3 L/min; I = 10 W/m^2).

two different initial NO concentration, which is also different from Devahasdin et al. [16].

Compared to undoped TiO_2, the cut-off wavelength of the carbon-doped TiO_2 extends to the visible bluish light range [25], which indicates the doped TiO_2 still has similar absorb ability in UV light range. Experiments were carried out to study the effect of the light wavelength in this study. Results are shown in Fig. 8, which is in accordance with Blöß and Elfenthal [25] who reported a 53.8% degradation rate with carbon-doped TiO_2 and 59.1% degradation rate with undoped TiO_2. The photocatalytic degradation effect of UV light is more than two times of that of the visible light in bluish green region with the same experimental conditions. However, as mentioned above, there is very little UV light irradiance in indoor air condition, so the combined effect of UV light and the visible light to activate the photocatalytic reaction remains an important open topic to apply the photocatalytic oxidation in indoor air conditions.

3.6. Effect of water vapor

Water plays a very important role in the photocatalytic oxidation because it produces the hydroxyl radical when combining with generated holes in the photocatalyst surface which then oxidizes NO into NO_2 and then to final product NO_3^-. Numerous studies have been carried out on its effect of the photocatalytic oxidation. Although the opinion that the competition between the pollutant and water adsorption onto the photocatalyst surface influences the PCO greatly is quite popular, no agreement has been obtained up to the authors' knowledge. Obee and Brown [1] reported the effect of the water vapor on the photocatalytic oxidation of three pollutants (toluene, formaldehyde, and 1,3-butadiene) is dependent on both humidity and initial pollutant concentrations, which can be explained as being a result of competitive adsorption on available hydroxyl adsorption sites and of changes in hydroxyl radical population levels. Kim and Hong [36] reported the influence of water vapor in photocatalytic oxidation depends on the species of pollutant. The effect of water on photocatalytic oxidation is also influenced by the substrate for the photocatalyst. Devahasdin et al. [16] reported that the conversion increases with the increase of the relative humidity from 0% until 50%, and then it becomes constant with NO as pollutant, using Pyrex as substrate. Wang et al. [20] reported a steady increase of the NO conversion with the increase of relative humidity from 8% until 100% using woven glass fabric as substrate for TiO_2. Ao and Lee [13] reported almost constant NO conversion with the increase of relative humidity from 10% until 70% using Teflon film as substrate. Beeldens [38] and Hüsken et al. [39] reported a steady decrease of the NO conversion with the increase of the relative humidity using concrete pavestone as substrate.

The effect of water on the photocatalytic oxidation was investigated by varying relative humidity from 10% to 70% since according to ASHRAE 30% to 60% of the relative humidity is recommended for a good indoor air quality. The experimental results are shown in Fig. 9. It is very clear that the NO_x conversion rate increases with the increase of the relative humidity, which is in line with Wang et al. [20]. The results indicate the problem of the competition between NO and water adsorption onto the photocatalyst surface does not exist at the low initial concentration used in the present study, which is also confirmed by Ao and Lee [13].

3.7. Effect of photocatalyst

Photocatalyst decides the photocatalytic oxidation reaction of NO. The generated electron and hole pairs promote the oxidation reaction with adsorbed pollutant and water on the photocatalyst surface. The effect of the photocatalyst amount was also studied in the present study since it influences the surface area which will result in different photocatalytic oxidation rates. In the present study, the dosage of the photocatalyst is based on the total weight of the investigated photocatalytic paper. Experimental results of the photocatalytic oxidation of NO with different dosages of the photocatalyst are shown in Fig. 10.

From the results it is obvious that the photocatalyst influences the photocatalytic oxidation rate greatly. The NO_x conversion increases linearly with the increase of the photocatalyst amount, which is in line with Hüsken et al. [39].

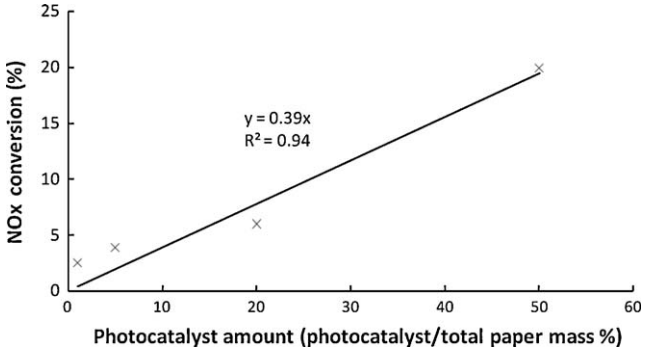

Fig. 10. Effect of the amount of photocatalyst on the NO_x conversion rate ($[C_{NO}]_{in}$ = 0.5 ppm; Q = 3 L/min; RH = 50%; I = 10 W/m^2).

4. Conclusion

This article addresses the air purification of indoor air pollutants using heterogeneous photocatalytic oxidation. A photocatalytic oxidation experimental set-up was developed for the present study with the ISO standard ISO 22197-1:2007 as a reference. To utilize the visible light in indoor air condition, a carbon-doped TiO_2 was chosen as photocatalyst using newly developed gypsum plasterboard cover paper as substrate. Using NO as target pollutant, the photocatalytic oxidation experiments were carried out in indoor air conditions.

The experimental results indicate that the photocatalytic oxidation is an effective air purification technology for indoor air pollutants. All photocatalytic oxidation experiments were carried out at room temperature under visible light which shows its convenience for the indoor air purification. Besides the photocatalyst, no other materials are required for the indoor air pollutants degradation.

Experimental conditions that affect the photocatalytic oxidation were investigated in detail in this study. Lower initial NO concentration shows a higher NO_x conversion, however, a longer reaction time is needed for the photocatalytic oxidation of NO with a very low initial concentration. Decreasing the volumetric flow rate of the pollutant results in a longer residence time, which in turn leads to a longer reaction time of the pollutant, which then leads to a higher NO_x conversion rate. The reactor becomes a batch reactor when the volumetric flow rate decreases to zero, which means a 100% of the conversion will be obtained given sufficient reaction time. Visible light was chosen as the light source for the photocatalytic oxidation of NO and the results show its validity. The NO_x conversion increases with the increase of the light intensity according to a logarithmic rule, which is different from the available literature so far. Furthermore, the effect of the light wavelength was studied and the NO_x conversion is more than two times higher in UVA region than in visible bluish region, which gives an open research topic of how to utilize the photocatalyst in indoor conditions more effectively. Water plays a very important role in the PCO because it is the source of the hydroxyl radical formation. Results do not show a competition between the water and pollutant adsorption onto the photocatalyst surface in the present study. Increasing the relative humidity results in a higher amount of the hydroxyl radical formation, which leads to a higher NO_x conversion. Photocatalytic oxidation of NO takes place on the photocatalyst surface, the higher the surface area of the photocatalyst is, the higher the NO_x conversion should be, which can be used to explain the higher NO_x conversion in this study when the amount of the photocatalyst increases.

The Langmuir–Hinshelwood model has been studied and applied to PCO extensively. And it was already applied successfully to describe the photocatalytic reaction rate of NO [32,40]. However, as an undesired intermediate, the behavior of NO_2 is seldom studied. Furthermore, the influence of the water is still an unclear factor to be modeled. The second part of this research will focus on the modeling of the photocatalytic oxidation of NO considering the influence of NO_2, the relation between reactants NO and water, and furthermore the effect of the light intensity.

Acknowledgements

The authors wish to express appreciations to Dipl.-Ing. M. Hunger and Dipl.-Ing. G. Hüsken for their previous work on the development of the PCO setup used in this study and help for the conduction of the experiments, and Dr. M.M. Ballari for the discussion and suggestions during the article composing, and their further gratitude to the European Commission (I-SSB Project, Proposal No. 026661-2) and the following sponsors of the research group: Bouwdienst Rijkswaterstaat, Rokramix, Betoncentrale Twenthe, Graniet-Import Benelux, Kijlstra Beton, Struyk Verwo Groep, Hülskens, Insulinde, Dusseldorp Groep, Eerland Recycling, ENCI, Provincie Overijssel, Rijkswaterstaat Directie Zeeland, A&G maasvlakte, BTE, Alvon Bouwsystemen, and v. d. Bosch Beton (chronological order of joining).

Appendix A. Supplementary data

Supplementary data associated with this article can be found, in the online version, at doi:10.1016/j.apcatb.2009.09.004.

References

[1] T.N. Obee, R.T. Brown, Environ. Sci. Technol. 29 (1995) 1223–1231.
[2] A.P. Jones, Atmos. Environ. 33 (1999) 4535–4564.
[3] A. Fujishima, K. Honda, Nature 238 (1972) 37–38.
[4] C.S. Kuo, Y.H. Tseng, C. Huang, Y. Li, J. Mol. Catal. A: Chem. 270 (2007) 93–100.
[5] B. Kraeutler, A.J. Bard, J. Am. Chem. Soc. 100 (1978) 4317–4318.
[6] W. Choi, A. Termin, M.R. Hoffmann, J. Phys. Chem. 98 (1994) 13669–13679.
[7] M. Anpo, Catal. Surv. Jpn. 1 (1997) 169–179.
[8] H. Yamashita, Y. Ichihashi, M. Takeuchi, S. Kishiguchi, M. Anpo, J. Synchrot. Radiat. 6 (1999) 451–452.
[9] R. Asahi, T. Morikawa, T. Ohwaki, K. Aoki, Y. Taga, Science 293 (2001) 269–271.
[10] T. Sano, N. Negishi, K. Uchino, J. Tanaka, S. Matsuzawa, K. Takeuchi, J. Photochem. Photobiol. A: Chem. 160 (2003) 93–98.
[11] M.R. Hoffmann, S.T. Martin, W. Choi, D.W. Bahnemann, Chem. Rev. 95 (1995) 69–96.
[12] K. Hashimoto, K. Wasada, M. Osaki, E. Shono, K. Adachi, N. Toukai, H. Kominami, Y. Kera, Appl. Catal. B: Environ. 30 (2001) 429–436.
[13] C.H. Ao, S.C. Lee, Appl. Catal. B: Environ. 44 (2003) 191–205.
[14] C.H. Ao, S.C. Lee, J. Photochem. Photobiol. A: Chem. 161 (2004) 131–140.
[15] C.H. Ao, S.C. Lee, J.C. Yu, J. Photochem. Photobiol. A: Chem. 156 (2003) 171–177.
[16] S. Devahasdin, C. Fan, J.K. Li, D.H. Chen, J. Photochem. Photobiol. A: Chem. 156 (2003) 161–170.
[17] H. Ichiura, T. Kitaoka, H. Tanaka, Chemosphere 51 (2003) 855–860.
[18] W.K. Jo, K.H. Park, Chemosphere 57 (2004) 555–565.
[19] R. Pelton, X. Geng, M. Brook, Adv. Colloid Interface Sci. 127 (2006) 43–53.
[20] H. Wang, Z. Wu, W. Zhao, B. Guan, Chemosphere 66 (2007) 185–190.
[21] B.N. Shelimov, N.N. Tolkachev, O.P. Tkachenko, G.N. Baeva, K.V. Klementiev, A.Y. Stakheev, V.B. Kazansky, J. Photochem. Photobiol. A: Chem. 195 (2008) 81–88.
[22] J.S. Dalton, P.A. Janes, N.G. Jones, J.A. Nicholson, K.R. Hallam, G.C. Allen, Environ. Pollut. 120 (2002) 415–422.
[23] International Organization for Standardization, ISO 22197-1:2007, Switzerland.
[24] J. Orth-Gerber, H. Kisch, Patent US 2005/0227857 A1, October 2005.
[25] S.P. Blöß, L. Elfenthal, in: Proceedings International RILEM Symposium on Photocatalysis Environment and Construction Materials-TDP, RILEM Publications, Bagneux, France, 2007, pp. 31–38.
[26] G. Hüsken, M. Hunger, H.J.H. Brouwers, in: Proceedings International RILEM Symposium on Photocatalysis Environment and Construction Materials-TDP, RILEM Publications, Bagneux, France, 2007, pp. 147–154.
[27] J.A. Hoskins, Indoor Built Environ. 12 (2003) 427–433.
[28] C.S. Turchi, D.F. Ollis, J. Catal. 122 (1990) 178–192.
[29] T.H. Lim, S.M. Jeong, S.D. Kim, J. Gyenis, J. Photochem. Photobiol. A: Chem. 134 (2000) 209–217.
[30] T. Maggos, J.G. Bartzis, M. Liakou, C. Gobin, J. Hazard. Mater. 146 (2007) 668–673.
[31] J. Zhao, X.D. Yang, Build. Environ. 38 (2003) 645–654.
[32] M. Hunger, H.J.H. Brouwers, in: Proceedings International Conference Excellence in Concrete Construction—through Innovation 2008, CRC Press, United Kingdom, 2008, pp. 545–552.
[33] A.V. Emeline, V. Ryabchuk, N. Serpone, J. Photochem. Photobiol. A: Chem. 133 (2000) 89–97.
[34] H. Yu, K. Zhang, C. Rossi, Indoor Built Environ. 16 (2007) 529–537.
[35] T.A. Egerton, C.J. King, J. Oil Chem. Assoc. 62 (1979) 386–391.
[36] J. Herrmann, Catal. Today 53 (1999) 115–129.
[37] S.B. Kim, S.C. Hong, Appl. Catal. B: Environ. 35 (2002) 305–315.
[38] A. Beeldens, in: Proceedings International RILEM Symposium on Photocatalysis Environment and Construction Materials-TDP, RILEM Publications, Bagneux, France, 2007, pp. 187–194.
[39] G. Hüsken, M. Hunger, H.J.H. Brouwers, Build. Environ. 22 (2009) 2463–2474.
[40] Q.L. Yu, H.J.H. Brouwers, M.M. Ballari, in: Proceedings the 3rd International Symposium on Nanotechnology in Construction, Springer-Verlag, Berlin Heidelberg, 2009, pp. 389–394.